

High resolution imaging of the GG Tau system at 267 GHz [★]

Vincent Piétu¹, Frédéric Gueth¹, Pierre Hily-Blant^{1,2}, Karl-Friedrich Schuster¹, and Jérôme Pety¹

¹ IRAM, 300 rue de la piscine, 38406 Saint Martin d'Hères, France

² LAOG, Université Joseph Fourier, CNRS, 38041 Grenoble, France

Received 2 September 2010/ Accepted 9 December 2010

ABSTRACT

Context. Studying circumbinary disks is critical to understanding the formation mechanisms of binary stars. While optical or mid-infrared images reveal the scattered emission, millimeter observations provide direct measurements of the dust thermal emission.

Aims. We study the properties of the circumbinary disk around the well-known, multiple young stellar object GG Tau with the highest possible sensitivity and spatial resolution.

Methods. We mapped the continuum emission of GG Tau at 267 GHz using the IRAM Plateau de Bure interferometer equipped with upgraded receivers and LO systems. An angular resolution of $0.45'' \times 0.25''$ was achieved, corresponding to a linear resolution of 65×35 AU.

Results. The GG Tau A circumbinary disk is observed as an extremely clearly defined narrow ring. The width of the ring is not resolved. Emission from the central binary is detected and clearly separated from the ring: it coincides with the GG Tau Aa position and may therefore trace a circumstellar disk around this star. The mass ratio of the circumbinary to circumprimary material is ~ 80 .

Key words. Stars: circumstellar matter - planetary systems: protoplanetary disks - individual: GG Tau - Radio-continuum: stars

1. Introduction

GG Tau is a well-known quadruple system located in the Taurus star-forming region. It is composed of two binaries, the northern one (GG Tau A) having been the subject of considerable attention during the past decade. This system, classified as a classical T Tauri star, is a close binary with a separation of ~ 35 AU (for an assumed distance of 140 pc). Its age is estimated to be 1.5 Myrs (White et al. 1999). GG Tau A is surrounded by a circumbinary disk, which has been extensively studied by means of its visible or mid-infrared scattered emission (e.g. Roddier et al. 1996; Silber et al. 2000; Krist et al. 2002; McCabe et al. 2002; Krist et al. 2005) and its direct thermal dust emission in the millimeter domain (e.g. Dutrey et al. 1994; Guilloteau et al. 1999). The higher angular resolution data clearly illustrate that the inner ~ 150 AU region of the disk has been emptied by tidal interactions with the two stars, making GG Tau one of the text-book example of circumbinary disk in young stellar systems.

Guilloteau et al. (1999) obtained kinematical information from ^{13}CO and HCO^+ lines, demonstrating that the disk is in Keplerian rotation (the redshifted emission being on the western side) around a $\sim 1.3 M_{\odot}$ system. These IRAM Plateau de

Bure observations also indicated that the circumbinary disk is composed of a ring with sharp edges ($\sim 70\%$ of the mass), surrounded by a more extended, colder disk. The total ring+disk mass is $\sim 0.12 M_{\odot}$. Interestingly, Guilloteau et al. (1999) noted the continuum 1.4 mm emission also revealed the presence of material *within* the ring, suggesting that there are circumstellar disks around the individual sources.

In this paper, we present new observations of the millimeter continuum emission of the GG Tau circumbinary disk, which provides a significant improvement in angular resolution and sensitivity compared to the Guilloteau et al. (1999) data and places new constraints on the properties of the circumbinary and primary disks.

2. Observations

During the winter 2007/2008, new local oscillator components for the 1 mm receiver band were installed on the Plateau de Bure Interferometer, enabling observations up to a frequency of 270 GHz (instead of 250 GHz previously). As part of the science verification program of this upgrade, GG Tau was observed in January–February 2008. The receivers were tuned in single side band at 267.2 GHz. Only one polarization channel was used, with a correlator setup covering a bandwidth of 2 GHz to enable the simultaneous observation of the $\text{HCN}(3-2)$ and $\text{HCO}^+(3-2)$ lines (which data will not be discussed in this article).

Send offprint requests to: Vincent Piétu, e-mail: pietu@iram.fr

[★] Based on observations carried out with the IRAM Plateau de Bure Interferometer. IRAM is supported by INSU/CNRS (France), MPG (Germany) and IGN (Spain).

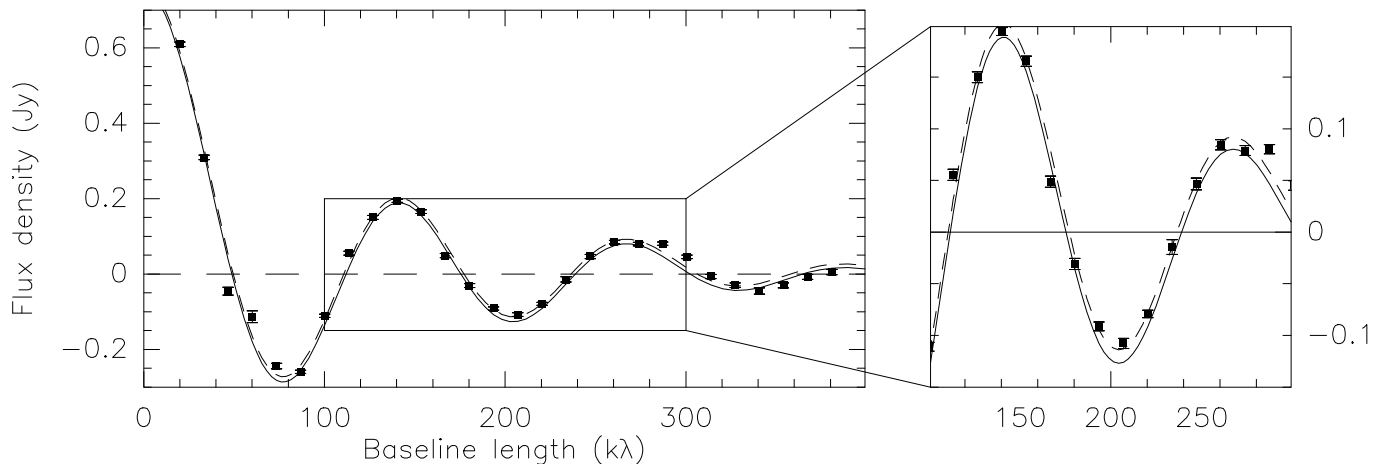


Fig. 1. Real part of the visibility v s baseline lengths. The points and error bars represent the measured values, and the curves are the best fits of a geometrical ring (plain curve; see Table 1) and of a ring plus a point source (dashed). The visibilities have been corrected from the disk orientation ($PA = 7^\circ$) and inclination ($i = 37^\circ$) by compressing the V value by $\cos(i)$ prior to circular averaging.

The source was observed with five antennas in the C configuration (baseline length from 25 to 175 m) and with six antennas in the A configuration (baseline length from 130 to 760 m). Both observations were done in track-sharing mode with two other sources, resulting in a six-antenna-equivalent total on-source integration time of 4 hours. The atmospheric conditions were excellent, with a water vapour content of 0.5–1 mm. This translated into a ~ 200 K system temperature around transit.

The data processing was performed with the GILDAS¹ software. Standard phase and amplitude calibration was applied to the data, using regular observations of the B0548+134 quasar. The atmospheric phase noise was $15\text{--}40^\circ$ for the C configuration and $30\text{--}50^\circ$ for the A configuration. The absolute flux calibration was performed using observations of MWC 349. Since this project was among the first Plateau de Bure observations at that high frequency, the flux density of MWC 349 was known only with a limited accuracy. We used an extrapolation of the measured flux densities at lower frequencies. We carefully checked the relative calibration of the two tracks by comparing the GG Tau flux density on the overlapping baselines. We estimate the final accuracy of the absolute flux density to be $\sim 20\%$.

The data were imaged using robust weighting, resulting in one of the highest angular resolutions achieved with the Plateau de Bure Interferometer, $0.45 \times 0.25''$ (at $PA 19^\circ$). At the distance of 140 pc, this corresponds to a linear resolution of 65×35 AU.

3. Results

The image reveals a very clear ring structure as well as an unresolved source located close to the ring center. We performed a fit of a geometrical ring of uniform brightness to the data, whose results are given in Table 1. They indicate a narrower ring than previous studies (Guilloteau et al. 1999), because of the increase in angular resolution. Fig. 1 displays the real part

¹ See <http://www.iram.fr/IRAMFR/GILDAS> for more information about GILDAS.

Ring observational parameters

	This work	Guilloteau et al. 1999
Frequency (GHz)	267	220
Ang. resolution('')	0.45×0.25	0.88×0.56
Flux (mJy)	760 ± 10	544 ± 3
Inner radius ('')	1.38 ± 0.01	1.27 ± 0.01
Outer radius ('')	1.84 ± 0.01	1.90 ± 0.01

Table 1. Parameters of a geometrical ring fitted to the uv data, and comparison with the results obtained with previous data.

of the circularly averaged visibilities as a function of the baseline length together with the visibility curve of the fitted ring, showing the excellent agreement with the data. A marginally tighter fit can be obtained by fitting a ring and a point source (Fig. 1, dashed curve).

In addition to standard imaging, we used a more sophisticated technique to optimize the imaging process for this dataset. The dirty beam of the observations had somewhat high sidelobes (at about 25% level), owing to the poor uv coverage of the compact C configuration. As a consequence, the emission within the (bright) ring was difficult to deconvolve properly. To overcome these difficulties, we subtracted from the visibilities the fitted geometrical ring (Table 1) and imaged and deconvolved separately the ring and the residual data. We then added the two deconvolved maps to obtain the final image presented in Fig. 2. The advantage of this method is the level of sidelobes caused by the bright ring structure is reduced and the dynamical range of the image is thus increased, especially in the inner part of the ring. On the final image, the peak brightness temperature is ~ 4 K, while the rms noise of the map is 1.6 mJy/beam (0.24 K), i.e. the dynamical range is > 15 .

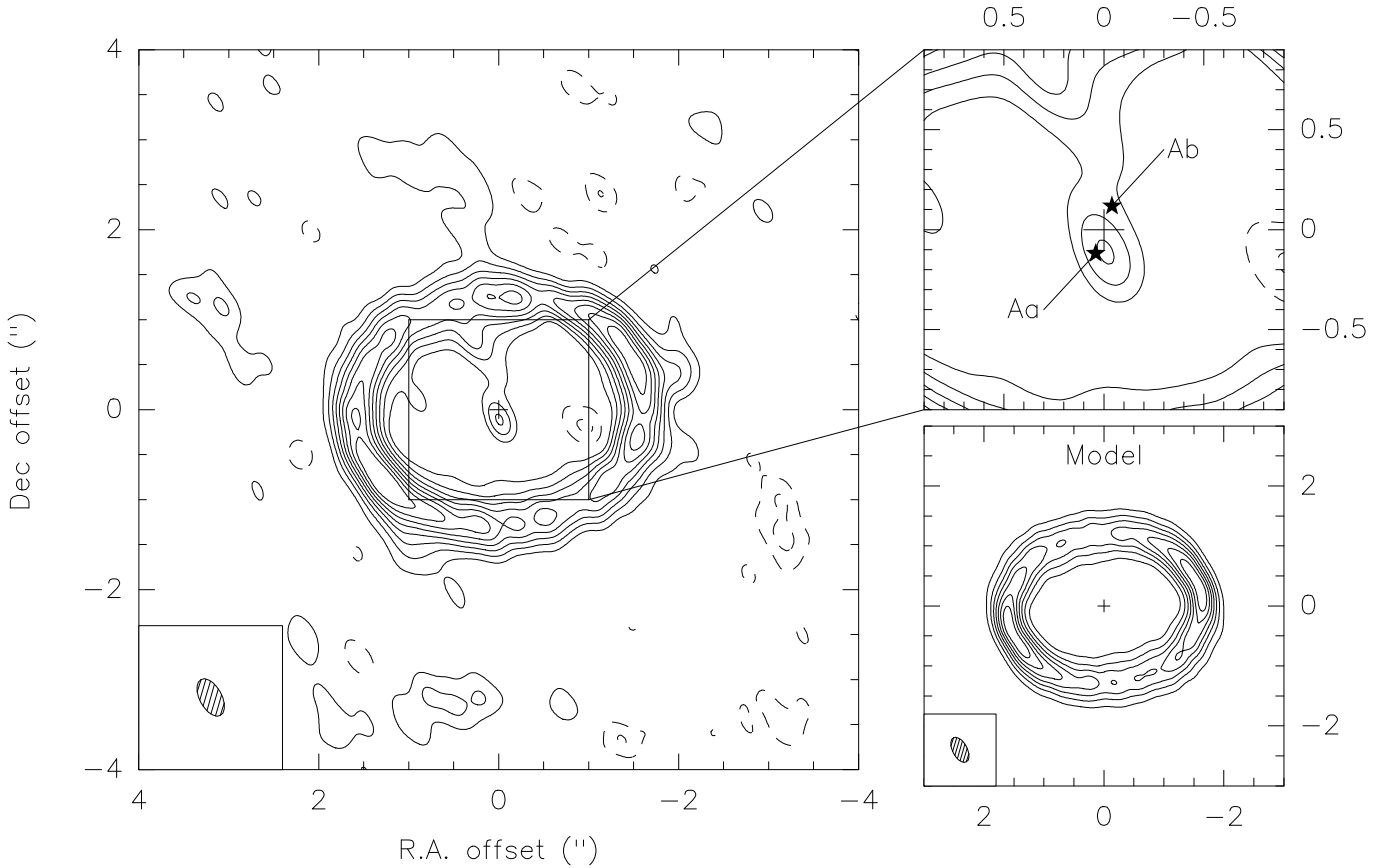


Fig. 2. **Left:** 267 GHz continuum image of GG Tau. The angular resolution is $0.45'' \times 0.25''$ at PA 19° , and the contour spacing is 3.1 mJy/beam (0.47 K, about 2σ). The map is centered at $\alpha = 04 : 32 : 30.356$, $\delta = 17 : 31 : 40.48$ (cross, J2000). The GG Tau B binary is located $\sim 10''$ towards the south, outside the plotted area. **Top right:** zoom of the inner $1''$ and position of the GG Tau A binary stars as of 2008. **Bottom right:** best physical ring model (see Table 2 and text). Angular resolution and contour spacing are as in the observations.

4. Data analysis

4.1. The ring

To analyse the continuum emission of the GG Tau circumbinary ring, we fitted a *physical* model of a ring (in contrast to the *geometrical* model mentioned in the previous section). From a parametric density and temperature description, the model solves for the radiative transfer to predict the observed emission, and performs a global χ^2 minimization directly in the uv plane (see e.g. Piétu et al. 2007, for a full description of the method). Here, the ring is assumed to be circular with a constant width and density. Its edges are modelled as Gaussians decreasing from the ring plateau. The model also includes a standard disk surrounding the ring, but its contribution is found to be negligible in reproducing these continuum data. Guilloteau et al. (1999) showed that $\sim 30\%$ of the mass lies in the outer disk, but our data lack short baseline measurements and are therefore certainly filtering out the disk extended emission.

Our best-fit results are presented in Table 2 and the corresponding image is displayed in Fig. 2. We could not constrain the kinetic temperature because the emission is optically thin within the ring and we therefore assumed a constant temperature of 35 K, as found from the optically thick

^{13}CO $J=2\rightarrow 1$ emission by Guilloteau et al. (1999). The derived inclination and position angle are in perfect agreement with those measured by Guilloteau et al. (1999). Compared to the results of these authors, the ring width is narrower (50 AU instead of 80 AU) and consequently the surface density has to be higher (2.2 instead of $1.4 \times 10^{24} \text{ cm}^{-2}$) in order to reproduce the observed flux density. The total mass derived from the model is $0.09 M_\odot$.

The ring width we measure remains only marginally resolved at the angular resolution of our observations, while the ring edges have a very narrow width (Gaussians $1/e$ widths < 10 AU), indicating a very sharp decrease in the density at the ring edges. Hence, the picture emerging is that of a very thin ring with a very pronounced overdensity compared to the inner and outer regions.

4.2. The central source

While Guilloteau et al. (1999) noted the presence of emission within the GG Tau ring, the data presented in this paper clearly separate for the first time the ring from the central emission. The central source that we detect is unresolved at the resolution of these observations (~ 50 AU). It is offset by $0.1'' \pm 0.1''$

Ring physical parameters	
Inclination (°)	37 ± 1
Position angle (°)	7 ± 1
Inner radius (AU)	200 ± 2
Outer radius (AU)	250 ± 2
Edge width (AU)	< 10
Temperature (K)	[35]
Temperature exponent	[0]
Surface density (cm^{-2})	$2.2 \pm 0.05 \times 10^{24}$
Surface density (g.cm^{-2})	9.6 ± 0.2
Dust emissivity κ (cm^{-2}/g)	[0.012]

Table 2. Fitted parameters of the GG Tau circumbinary ring. Error bars are 1σ formal errors, not taking into account phase noise nor flux calibration uncertainty. Square brackets indicate fixed parameters.

in R.A. and $-0.1'' \pm 0.1''$ in declination from the ring center position and has a flux density of 10 mJy, i.e. a brightness temperature of 1.4 K in our synthesized beam.

Using orbital parameters derived by Beust & Dutrey (2005) for the inner binary, we extrapolated the position of the stars at the time of the observations, i.e. beginning of 2008. These positions ($0.25''$ separation, -19° separation angle) are indicated in the top right panel of Fig. 2. The absolute astrometry of the stars not being known with enough precision, we forced the center of mass of the binary (the two stars have similar masses, $0.78 M_\odot$ and $0.68 M_\odot$, White et al. 1999) to coincide with the geometrical center of the ring (cross in Fig. 2). This hypothesis would not be correct if the ring were elliptical: the center of mass would then be at one of the ellipse foci. The data and models do however indicate the ring is circular at our angular resolution. With these assumptions, the inner continuum emission is clearly associated with the binary stars. It is thus tempting to identify this source with the thermal dust emission of one or two circumstellar disks around the individual stars (an alternative, although less probable origin would be free-free emission from an ionized jet).

The continuum emission seems to peak at GG Tau Aa, although the formal fitted position indicates a marginal result (2.5σ). Both stars exhibit optical emission lines that are typical of classical T Tauri stars and trace accretion processes (White et al. 1999), hence indicate that both sources should have an accretion disk. Our observations suggest that the millimeter continuum emission of the GG Tau Ab disk is weaker than that of the Aa disk, by at least a factor of 3, which points towards a less massive and/or colder disk. This is consistent with GG Tau Ab displaying weaker emission lines than Aa (White et al. 1999), which is indicative of less intense accretion activity.

A disk around GG Tau Aa would be truncated by the relative motion of Ab to a size typically one third of the orbital distance, i.e. ~ 10 AU. Correcting for beam dilution, the brightness temperature can thus be ~ 30 K, which is a lower limit to the disk kinetic temperature T_{kin} . The corresponding mass, assuming optically thin emission, would be $1.5 \cdot 10^{-3} M_\odot$ (scaling with $30 \text{ K}/T_{\text{kin}}$).

4.3. Streamer?

The image of GG Tau presented in this paper also reveals a continuous structure connecting the northern part of the circumbinary disk with the central source. It is very suggestive of a streamer feeding matter onto the central individual disk(s), as suggested by a number of theoretical models of circumbinary disk evolution (e.g. Artymowicz & Lubow 1996). We note however that this structure is only marginally detected in our observation (contours are 2σ in Fig. 2) so that it is difficult to draw firm conclusions about its existence.

Fig. 2 also shows several other low-level (one contour) extensions of the ring. The reality of these structures remains to be confirmed, since they are close to the noise level and may also correspond to deconvolution artefacts in the imaging process. We note, however, that the position of the feature at the external edge of the south-east portion of the ring coincides with the 'kink' seen in NIR scattered emission by Silber et al. (2000) or McCabe et al. (2002). Similarly, the western-most extension is seen with several contours, and may trace a local enhancement of the column density, which could explain the western part of the ring being brighter at lower frequency (3.4 mm, Guilloteau et al. 1999 or 2.7 mm, Dutrey et al. 1994).

Finally, the apparent clumpy structure of the ring is not significant: all peaks correspond to a $< 2\sigma$ difference with a uniform ring, as for instance in the model shown in the right part of the figure.

5. Summary

We have presented a map of the 267 GHz continuum emission in GG Tau A, at the unprecedented angular resolution of $0.45 \times 0.25''$, i.e. 65×35 AU at the distance of Taurus. These observations confirm the previous findings of Guilloteau et al. (1999) but allow us to place more accurate constraints on the properties of this system. Our main conclusions are:

- The circumbinary dust emission is confined to a circular ring of width < 50 AU, with very pronounced sharp edges. These observations place very tight constraints on theoretical model of the dynamical processes leading to the formation of rings in circumbinary systems (e.g. Beust & Dutrey 2005, 2006). GG Tau is 1.5 Myrs old, but, as noted by Beust & Dutrey (2006), the observed ring may be a transient feature that will undergo significant evolution in the next Myrs.
- The data very clearly differentiate the circumbinary disk from the emission located within the disk: an unresolved source is detected at the position of GG Tau Aa. This could be the first direct detection of a circumstellar disk surrounding one of the stars of the central binary system. The mass of the circumprimary disk(s) is $1.5 \cdot 10^{-3} M_\odot$, about 80 times less than the mass of the circumbinary material.

These observations confirm that GG Tau A is one of the best known and most interesting examples of a disk surrounding a young binary T Tauri system. It will be a prime target for future high angular studies with an instrument like ALMA.

Acknowledgements. We acknowledge help from the Plateau de Bure staff for performing the observations.

References

- Artymowicz, P. & Lubow, S. H. 1996, *ApJ*, 467, L77+
- Beust, H. & Dutrey, A. 2005, *A&A*, 439, 585
- Beust, H. & Dutrey, A. 2006, *A&A*, 446, 137
- Dutrey, A., Guilloteau, S., & Simon, M. 1994, *A&A*, 286, 149
- Guilloteau, S., Dutrey, A., & Simon, M. 1999, *A&A*, 348, 570
- Krist, J. E., Stapelfeldt, K. R., Golimowski, D. A., et al. 2005, *AJ*, 130, 2778
- Krist, J. E., Stapelfeldt, K. R., & Watson, A. M. 2002, *ApJ*, 570, 785
- McCabe, C., Duchêne, G., & Ghez, A. M. 2002, *ApJ*, 575, 974
- Piétu, V., Dutrey, A., & Guilloteau, S. 2007, *A&A*, 467, 163
- Roddier, C., Roddier, F., Northcott, M. J., Graves, J. E., & Jim, K. 1996, *ApJ*, 463, 326
- Silber, J., Gledhill, T., Duchêne, G., & Ménard, F. 2000, *ApJ*, 536, L89
- White, R. J., Ghez, A. M., Reid, I. N., & Schultz, G. 1999, *ApJ*, 520, 811